1146 *Biochemistry* **2010,** *49,* 1146–1159
DOI: 10.1021/bi901247h

BIOCHEMISTRY
including biophysical chemistry & molecular biology
Article

The Influence of Hydrogen Bonds on the Electronic Structure of Light-Harvesting Complexes from Photosynthetic Bacteria†

G. Uyeda,‡ J. C. Williams,‡ M. Roman,§ T. A. Mattioli,§ and J. P. Allen*,‡

‡*Department of Chemistry and Biochemistry, Arizona State University, Tempe, Arizona 85287-1604, and* §*Service de Bioénergétique, Département de Biologie Joliot Curie, CEA Saclay, 91191 Gif-sur-Yvette Cedex, France*

Received July 21, 2009; Revised Manuscript Received December 23, 2009

ABSTRACT: The influence of hydrogen bonds on the electronic structure of the light-harvesting I complex from *Rhodobacter sphaeroides* has been examined by site-directed mutagenesis, steady-state optical spectroscopy, and Fourier-transform resonance Raman spectroscopy. Shifts of 4−23 nm in the Q_y absorption band were observed in seven mutants with single or double changes at Leu α44, Trp α43, and Trp *β*48. Resonance Raman spectra were consistent with the loss of a hydrogen bond with the alteration of either Trp α43 or Trp *β*48 to Phe. However, when the Trp α43 to Phe alteration is combined with Leu α44 to Tyr, the spectra show that the loss of the hydrogen bond to α43 is compensated by the addition of a new hydrogen bond to Tyr α44. Comparison of the absorption and vibrational spectra of the seven mutants suggests that changes in the absorption spectra can be interpreted as being due to both structural and hydrogen-bonding changes. To model these changes, the structural and hydrogen bond changes are considered to be independent of each other. The calculated shifts agree within 1 nm of the observed values. Excellent agreement is also found assuming that the structural changes arise from rotations of the C3-acetyl group conformation and hydrogen bonding. These results provide the basis for a simple model that describes the effect of hydrogen bonds on the electronic structures of the wild-type and mutant light-harvesting I complexes and also is applicable for the light-harvesting II and light-harvesting III complexes. Other possible effects of the mutations, such as changes in the disorder of the environment of the bacteriochlorophylls, are discussed.

The photosynthetic unit of purple bacteria is composed of three integral membrane proteins: the reaction center, a core light-harvesting I complex (LH1),[1] and in many bacteria a peripheral light-harvesting II (LH2) complex (*1*). All three complexes of the photosynthetic unit of *Rhodobacter sphaeroides* contain the same pigment, bacteriochlorophyll (BChl) *a*, but within these three complexes, this pigment gives rise to absorption bands with maxima at 800 and 850 nm in LH2 and 875 nm in LH1. The means by which the protein environment tunes the absorption bands of this cofactor in antenna complexes has long been a topic of study (*2*−*5*). The proposed mechanisms include distortions to the planar conformation of the macrocycle, excitonic coupling between closely spaced pigments, rotation of the C3-acetyl group, and hydrogen bonding to the carbonyl groups conjugated to the delocalized electronic structure of the macrocycle. By altering certain residues using site-directed mutagenesis and correlating shifts in the absorption spectrum with shifts of the vibrational bands attributed to these carbonyl groups in the Fourier-transform resonance Raman spectrum, an understanding of the importance of hydrogen bonding can be established.

Atomic level information for the photosynthetic proteins in the purple bacterial photosynthetic unit comes from the three-dimensional structures of the reaction centers from *Rb. sphaeroides* and *Blastochloris viridis* (*6*, *7*), the LH2 complexes from *Rhodopseudomonas acidophila* and *Rhodospirillum molischianum* (*8*, *9*), and a spectroscopic variant of the LH2 complex from *Rps. acidophila* called the light-harvesting III (LH3) complex (*10*). The LH2 and LH3 three-dimensional structures show eight or nine protomeric complexes arranged in a symmetrical ring configuration (Figure 1A). Each protomeric complex is made up of two peptides, α and *β*, three BChl *a* molecules, and at least one carotenoid molecule. Two of these BChl molecules are positioned near the periplasmic side of the membrane and are closely spaced with their ring planes perpendicular to the membrane in a manner similar to the arrangement observed for the BChls that make up the primary donor in reaction centers. The third is located closer to the cytoplasmic side of the membrane and oriented with its plane closer to parallel with the membrane. The circular arrangement of the individual units results in the overlapping of the closely spaced pair of BChl molecules with similar BChls from neighboring units. The resulting complex has 16 or 18 overlapping BChl molecules whose close proximity forms an aggregate of excitonically coupled pigments that collectively give rise to an absorption band near 850 nm and eight or nine monomeric BChl molecules that have an absorption band near 800 nm.

The LH1 complex has a similar ring arrangement of 16 protomeric complexes (Figure 1B), but current studies lack the resolution to provide a detailed picture. Projection maps from electron micrographs of two-dimensional crystals of LH1 from *Rhodospirillum rubrum* are consistent with a composition of two peptides, α and *β*, two BChl *a* molecules, and one carotenoid molecule arranged in a manner similar to that seen in LH2 but lacking the third monomeric BChl (*11*). Structural studies of LH1 from different species have shown that the circular architecture observed in *Rsp. rubrum* is probably not typical of LH1 in other species (*3*, *4*). In *Rb. sphaeroides* and *Rhodobacter capsulatus*,

†This work was supported by Grant MCB 0640002 from the NSF.
*To whom correspondence should be addressed. Phone: 480-965-8241. Fax: 480-965-2747. E-mail: jallen@asu.edu.
[1]Abbreviations: LH1, light-harvesting I complex; LH2, light-harvesting II complex; LH3, light-harvesting III complex; BChl, bacteriochlorophyll.

 Published on Web 01/12/2010

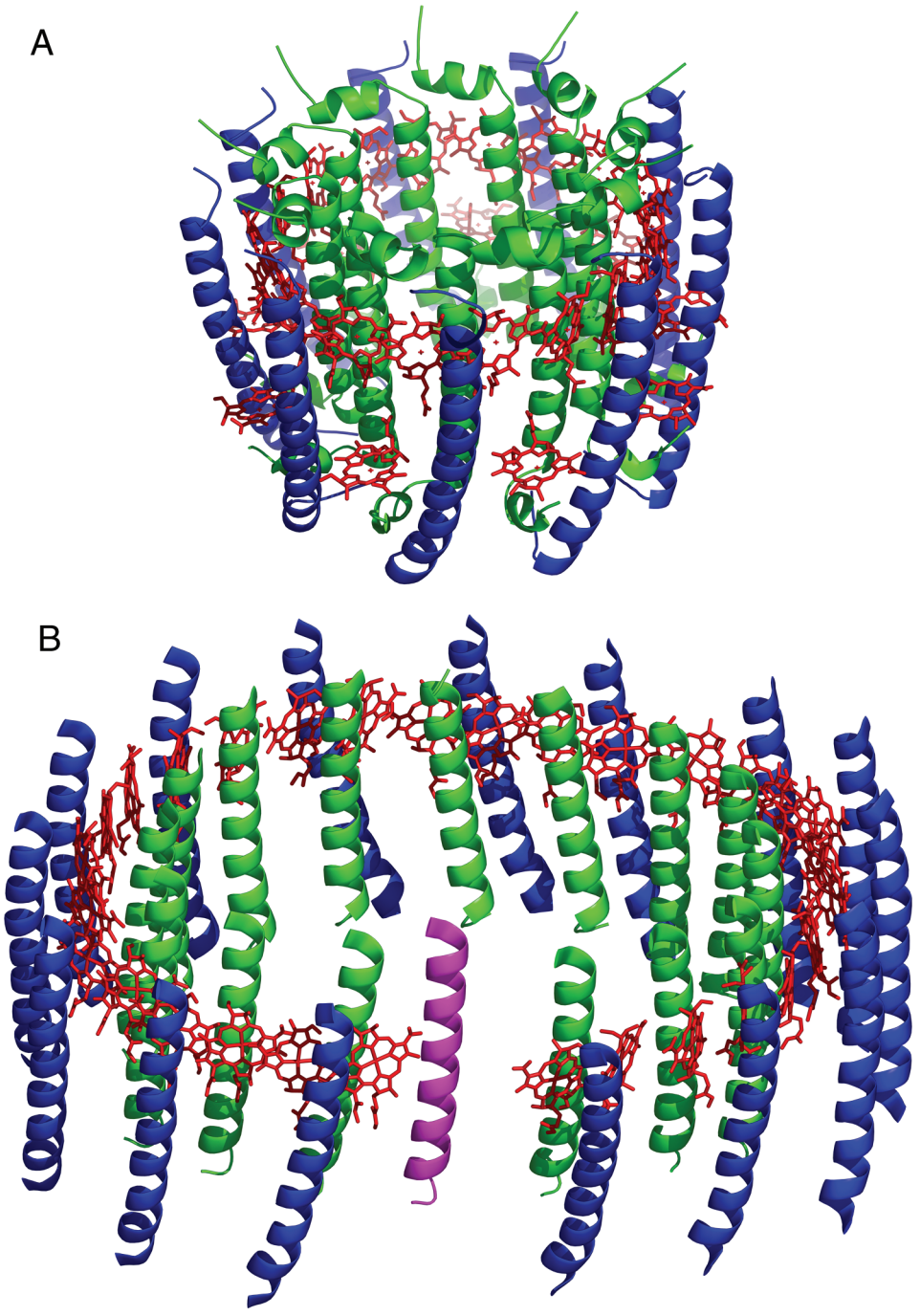

FIGURE 1: (A) Three-dimensional structure of the LH2 complex from *Rps. acidophila* showing the backbones of the α subunits (green) forming the inner ring and the *β* subunits (blue) forming the outer ring and the BChls (red) forming two sets of rings. The carotenoids are not shown. The structure is from McDermott and co-workers (*8*), file 1KZU.pdb. (B) Low-resolution three-dimensional structure of the LH1 complex from *Rps. palustris* showing the backbones of the α subunits (green) forming the inner ring and the *β* subunits (blue) forming the outer ring, the putative *pufX* protein (purple), and the BChls (red) forming one ring. The carotenoids are not shown. The structure is from Roszak and co-workers (*19*), file 1PYH.pdb.

the PufX protein has been proposed to be part of the LH1 complex (*12*−*15*). The disruption of a symmetrical arrangement of LH1 is supported by atomic force microscopy that has revealed elliptical LH1 complexes in *Rb. sphaeroides* (*16*, *17*) as well as other organisms (*18*). Additional support is provided by a low-resolution model of LH1 from *Rhodopseudomonas palustris* (Figure 1B) that shows an ellipse broken because of the presence of a third polypeptide (*19*). While understanding of the quaternary structure of the LH1 complex continues to develop, the protomeric complexes from which they are assembled are believed to be structurally similar to those found in the LH2 complexes with the absence of the B800 BChl. In particular, the similarity between the sequences of the LH2 complex from *Rsp. molischianum* and the LH1 complex of *Rb. sphaeroides* (*20*) has led to the use of this LH2 structure as a model for the protomeric complex of the LH1 complex.

In the LH1 complex of *Rb. sphaeroides*, the hydrogen bond donors are believed to be Trp α43 and Trp *β*48. Replacing Trp *β*48 with Phe results in the loss of a hydrogen bond and a 6 nm blue shift in the absorption spectrum (*21*), while replacing Trp α43 with Phe results in a similar loss of a hydrogen bond but a much larger 24 nm blue shift (*22*). However, this latter shift is not believed to be solely the result of the loss of the hydrogen bond, as replacing Trp α43 with Tyr maintains the hydrogen bond but the

mutant still exhibits a 12 nm blue shift with respect to wild type (*22*). The 12 nm difference between the Trp α43 to Phe mutant and the Trp α43 to Tyr mutant was interpreted as being more representative of the effect of the loss of the hydrogen bond, with the remainder of the difference relative to wild type being due to some other factor, such as a structural change. Slightly larger shifts of approximately 16 nm have been reported for mutations in LH2 that alter the hydrogen bonding to the B850 BChls (*23*−*25*), and an approximately 10 nm shift has been reported for mutations that alter the hydrogen bonding to the B800 BChls (*26*). All of these shifts are similar to a theoretical hydrogen bond effect of 101.5 cm^{-1}, which at these wavelengths corresponds to a shift of approximately 7 nm, calculated for a monomeric BChl *a* molecule (*27*).

The relationship between hydrogen bonds and optical shifts became less clear with the determination of the three-dimensional structure of the LH3 complex of *Rps. acidophila* (*10*). This complex exhibits a dramatically blue-shifted absorption band at 820 nm relative to the 850 nm band for the LH2 complex. Prior to the structure determination, a comparison of the sequences and resonance spectra of the two complexes, along with the spectral shifts observed for the LH1 and LH2 mutants, implicated the lack of hydrogen bonds in the LH3 complex as a potential reason for the blue shift (*28*). The three-dimensional structure of LH3 shows that only one of the BChls associated with the 850 nm band lacks a hydrogen-bonded acetyl group, while the other maintains it through a Tyr residue at position α41. Both of the BChls in the three-dimensional structure of LH3 associated with the 850 nm band show a dramatic rotation of the acetyl groups away from the plane of the BChl macrocycle. This large conformational difference along with the maintenance of one of the hydrogen bonds indicates that the spectral difference between the LH2 and LH3 complexes is more likely to be the result of the increase of the dihedral angles for the C3-acetyl groups rather than the decrease in the number of hydrogen bonds to the acetyl groups.

This comparison of the LH2 and LH3 complexes raises the question of the relative importance of structural differences in the shifts in the spectra of the *Rb. sphaeroides* LH1 and LH2 mutants. Structural differences almost certainly contribute to the large shift observed for the mutant LH1 complex with Trp α43 replaced by Phe, but the extent to which structural changes affect the observed shifts for other LH mutants is unclear. In earlier work, the substitution of Trp α43 with Phe was associated with possible perturbation of the excitonic interactions between the BChls (*22*) or rearrangement of the BChls (*21*). The differences in the angle of the acetyl group when comparing the LH2 and LH3 complexes provide a specific type of structural change that is expected to alter the transition energy of the individual BChl pigments but not the coupling between the BChl molecules (*29*). Thus, the relationship between the electronic structure of the BChls and the observed transition energy is not simple, and in particular it is not clear why changes in hydrogen bonding should produce similar optical shifts for the monomeric and coupled BChls.

This paper reports the characterization of seven mutants of the LH1 complex of *Rb. sphaeroides* with alterations at residues α43, α44, and *β*48. Optical spectra in isolated LH1 complexes were measured using steady-state optical spectroscopy, and the hydrogen-bonding patterns of the BChls were determined using Fourier-transform resonance Raman spectroscopy. Different approaches were taken to differentiate the structural and hydrogen-bonding contributions to the observed shifts in the absorption spectrum. One approach used a fitting procedure to interpret the observed spectral differences between several LH1 mutants in terms of structural and hydrogen-bonding contributions. Another approach estimated the effect of hydrogen bonding and acetyl group conformation on the site energy of the BChl pigments with the effect of excitonic coupling explicitly included. The consistency of the two approaches is discussed as well as the general impact of hydrogen bonding on the spectral features of light-harvesting complexes.

MATERIALS AND METHODS

Mutagenesis and Protein Isolation. The seven LH1 mutants described in this paper were constructed from four mutated α genes, one mutated *β* gene, and the wild-type α and *β* genes. The four mutated α genes code for four mutant α-peptides with the following changes: Trp α43 to Phe, Leu α44 to Tyr, Leu α44 to Phe, and a double mutant, Trp α43 to Phe and Leu α44 to Tyr. One mutation was made in the *β* gene resulting in the change of Trp *β*48 to Phe. The mutants were named on the basis of the amino acid residues at positions α43, α44, and *β*48. Thus the effects of changes at these positions can be compared in the seven mutants, WYW (Trp α43, Tyr α44, Trp *β*48), WFW (Trp α43, Phe α44, Trp *β*48), WLF (Trp α43, Leu α44, Phe *β*48), WYF (Trp α43, Tyr α44, Phe *β*48), WFF (Trp α43, Phe α44, Phe *β*48), FYW (Phe α43, Tyr α44, Trp *β*48), and FLW (Phe α43, Leu α44, Trp *β*48), and the wild-type WLW (Trp α43, Leu α44, Trp *β*48). All of the possible combinations of α43 (Phe or Trp), α44 (Leu, Phe, or Tyr), and *β*48 (Phe or Trp) were constructed, but the four mutants with Phe substituted at both α43 and α44 or *β*48 (FLF with Phe α43, Leu α44, Phe *β*48, FFF with Phe α43, Phe α44, Phe *β*48, FFW with Phe α43, Phe α44, Trp *β*48, and FYF with Phe α43, Tyr α44, Phe *β*48) did not produce detectable amounts of LH1 in membrane preparations and are not considered in this paper.

Mutagenesis was performed on templates in the vector pUC19 (*30*) containing the individual LH1 α or *β* gene, using either a PCR technique or a variant of the procedure employed by the commercially available QuikChange mutagenesis kit (Stratagene). The PCR technique used a mutagenic oligonucleotide and either a forward or reverse sequencing primer to generate a mutated gene fragment containing restriction sites that allowed transfer of the mutated segment back into the template plasmid. The first step in the second technique was performing a PCR reaction using a mutagenic oligonucleotide and a reverse sequencing primer to generate a mutant gene fragment. Unlike the PCR technique described above, this fragment did not contain suitable restriction sites that would allow its easy transfer back into one of the template plasmids. Instead, this double-stranded gene segment was substituted for the double-stranded mutagenic oligonucleotide construct in the procedure utilized by the QuikChange mutagenesis kit.

The mutated genes were combined either with each other or with the wild-type genes to form pUC19-based constructs containing both α and *β* genes. These mutant LH1 sequences were transferred to the plasmid pLH30, based on pRK415 (*31*). This plasmid contains the *puf* operon with two substantial modifications: the replacement of the *puf*B to *puf*A segment with a kanamycin resistance cassette and the deletion of a *Kpn*I-*Kpn*I fragment of the *puf*L gene. The deletion in the *puf*L gene prevents assembly of the photosynthetic reaction center. Transfer of the fragment containing the mutated LH1 sequence replaces the kanamycin resistance cassette and produces a vector capable of expressing the mutant LH1 complexes without the reaction center. The plasmids were transformed into *Escherichia coli* S17-1 (*32*) and conjugated to the *Rb. sphaeroides* strain ΔBALM, which is incapable of expressing the reaction center, LH1,

and LH2 complexes (*33*). Wild-type LH1 was obtained from the *Rb. sphaeroides* strain ΔRC-1A, which contains a plasmid coding for the wild-type LH1 α and β subunits but includes the deletion in the gene encoding the reaction center L subunit.

Mutant strains were grown semiaerobically in the dark at 30 °C for 3 days. Harvested cells were resuspended in 15 mM Tris·HCl, pH 8, and 1 mM EDTA, and fragmented by either sonication (Branson) or using a French press (SLM Instruments). The resulting lysate was cleared by centrifugation for 10 min at 9000*g* and 4 °C in a Sorvall R5 centrifuge. Chromatophores were isolated from the resulting supernatant by centrifugation for 2 h at 184000*g* and 4 °C in a Beckman L7 centrifuge. The pelleted chromatophores were resuspended in 15 mM Tris·HCl and 1 mM EDTA, pH 8. LH1 complexes were extracted from the membranes using a variant of a procedure described previously (*34*). The complexes were solubilized using 0.5−1.0% lithium dodecyl sulfate with the detergent concentration adjusted depending upon the level of LH1 in the membrane. In addition, the complexes were independently isolated using the detergent octyl β-glucoside at concentrations of 0.5−1.0%. After solubilization, membranes were removed by ultracentrifugation for 2 h at 184000*g* and 4 °C in a Beckman L7 centrifuge. Excess detergent was removed by adding solid KCl to the resulting supernatant to achieve a final concentration of 15 mM. After 15 min of stirring on ice, the precipitated detergent was removed by centrifugation for 10 min at 20000*g* and 4 °C. The resulting supernatant was brought to 2% ammonium acetate and stirred on ice for 15 min. After 10 min of centrifugation at 20000*g* and 4 °C, the pelleted LH1 complexes were resuspended in 15 mM Tris·HCl, 1 mM EDTA, pH 8, and 0.05% lithium dodecyl sulfate (or 0.8% octyl β-glucoside). Resuspended complexes were subjected to two cycles of centrifugation for 2 h at 184000*g* and 4 °C in a Beckman L7 centrifuge and resuspension in 15 mM Tris·HCl, 1 mM EDTA, pH 8, and 0.05% lithium dodecyl sulfate (or 0.8% octyl β-glucoside).

Size-Exclusion Chromatography. The sizes of the purified complexes were estimated by use of size-exclusion chromatography with a Sephacryl HR 200 column (Amersham) in 15 mM Tris·HCl, 0.1% Triton X-100, and 1 mM EDTA. Measurement of each sample was performed three to five times. In addition to standard water-soluble proteins, the column was calibrated using LH2 and reaction centers from *Rb. sphaeroides*.

Optical Spectroscopy. Steady-state optical absorption spectra were measured using a Cary 5 spectrophotometer (Varian). Because several of the detergent-solubilized mutant complexes were not very stable at room temperature, samples were maintained at 8 °C during the measurement by use of a jacketed cuvette holder cooled by water flow from a refrigerated, circulating water bath (Haake).

Fourier-Transform Resonance Raman Spectroscopy. Fourier-transform resonance Raman spectra were recorded using a Bruker IFS 66 interferometer equipped with a liquid nitrogen-cooled Ge detector, which was coupled to a Bruker FRA Raman module equipped with a continuous diode-pumped Nd:YAG laser providing 1064 nm excitation, in preresonance with the approximately 870−880 nm absorption band, as described elsewhere (*35*). LH1 samples were concentrated using MicroCon (Amicon) concentrators with a 10 kDa cutoff membrane. Approximately 7 μL of the samples was deposited into aluminum cups that were kept on ice prior to measurements. The samples were covered with a glass coverslip to prevent sample evaporation and were measured using a 180° backscattering geometry for 15 min, and then the sample was changed for a fresh one in another precooled aluminum cup. This procedure was repeated until the averaged spectrum was of the desired quality; the spectra reported here are the averages of 2000−5000 coadded interferograms. Laser power was 250 mW, and the spectral resolution was 4 cm^{-1}. The Raman signals were carefully monitored during initial 15 min trials, and no evolution of the Raman spectra was observed during the measurements. Buffer spectra were also recorded under similar conditions and were subtracted from the sample spectra. A linear baseline was fit to valley regions common in all of the sample spectra from 500 to 1800 cm^{-1} and subtracted to reduce the visual effect of the slope resulting from the instrument response.

Excitonic Calculations. To evaluate the effect of the mutations on the coupling, changes made to the amino acid sequence were interpreted as affecting the site energy of the α- and β-bound BChl molecules. Evaluating the effect of these changes on the Q_y transition of the LH complex requires using those altered site energies in a calculation that takes into account the excitonic coupling of the BChl molecules in the complex. The most accessible approach to doing this type of calculation is the use of an effective Hamiltonian provided by Hu and co-workers (*36*). Their approach utilizes the three-dimensional structure of LH2 from *Rsp. molischianum*, but one of the key advantages of the effective Hamiltonian approach is its easy extensibility to several systems. The Hamiltonian itself has been applied to nonsymmetrical LH1 models incorporating PufX (*37*) but is more accessible if the symmetric case is taken. In this treatment, the complex is considered to be a symmetric arrangement of α/β dimers with perfect C_N symmetry with any effects due to asymmetry assumed to be minor. For evaluation of the LH1 complexes, coordinates were taken from Hu and coworkers (*36*), and for the LH2 and LH3 complexes the coordinates of the *Rps. acidophila* LH2 (1KZU.pdb) (*8*) were transformed to achieve a three-dimensional structure with C_9 symmetry. Calculation of the Q_y transition energy does not include any consideration of diagonal disorder.

An idealized LH complex with C_N symmetry can be represented by the Hamiltonian:

$$\hat{H} = \begin{pmatrix} \varepsilon_\alpha & \nu_1 & W_{1,3} & W_{1,4} & \cdots & W_{1,2N-2} & W_{1,2N-1} & \nu_2 \\ \nu_1 & \varepsilon_\beta & \nu_2 & W_{2,4} & \cdots & W_{2,2N-2} & W_{2,2N-1} & W_{2,2N} \\ W_{3,1} & \nu_2 & \varepsilon_\alpha & \nu_1 & \cdots & W_{3,2N-2} & W_{3,2N-1} & W_{3,2N} \\ W_{4,1} & W_{4,2} & \nu_1 & \varepsilon_\beta & \cdots & W_{4,2N-2} & W_{4,2N-1} & W_{4,2N} \\ \cdots & \cdots & \cdots & \cdots & \cdots & \cdots & \cdots & \cdots \\ W_{2N-2,1} & W_{2N-2,2} & W_{2N-2,3} & W_{2N-2,4} & \cdots & \varepsilon_\beta & \nu_2 & W_{2N-2,2N} \\ W_{2N-1,1} & W_{2N-1,2} & W_{2N-1,3} & W_{2N-1,4} & \cdots & \nu_2 & \varepsilon_\alpha & \nu_1 \\ \nu_2 & W_{2N,2} & W_{2N,3} & W_{2N,4} & \cdots & W_{2N,2N-2} & \nu_1 & \varepsilon_\beta \end{pmatrix} \quad (1)$$

where ε_α and ε_β are the individual transition energies, or site energies, of the α- and β-bound BChl, respectively. The nearest-neighbor intra- and interdimer couplings are given by ν_1 and ν_2, respectively. All other matrix elements

are determined by the dipole−dipole coupling interaction:

$$W_{i,j} = C\left[\frac{d_i \cdot d_j}{|R_{i,j}|^3} - \frac{3(d_i \cdot R_{i,j})(d_j \cdot R_{i,j})}{|R_{i,j}|^5}\right] \quad (2)$$

where d_i and d_j are unit vectors parallel to the transition dipole moments of the ith and jth BChls in the complex, respectively. The parameter $R_{i,j}$ represents the vector pointing from the central Mg of the ith BChl to the central Mg of the jth BChl, and $|R_{i,j}|$ is the magnitude of this vector, or the distance between two Mg atoms. The scaling parameter C is given by the product of the transition dipole moments for the ith and jth BChl, μ_i and μ_j, and the dielectric constant, ε, within the complex:

$$C = \frac{|\mu_i||\mu_j|}{4\pi\varepsilon} \quad (3)$$

Because of the symmetry of the complex, the diagonalization of this matrix can be done algebraically (*36*) and results in $2N$ eigenvalues: two for each value of $n = 1, 2, 3, ..., N$, each of which corresponds to an energy value for a level in the excitonic manifold. The value for each of these eigenvalues is given by

$$E_{n,\pm} = \frac{\varepsilon_\alpha + \varepsilon_\beta}{2} + \frac{1}{2}\left(\sum_{k=1}^{N-1} X_{k+1,n}(W_{1,2k+1} + W_{2,2k+2})\right) \pm \left\{\frac{1}{4}\left[\varepsilon_\alpha - \varepsilon_\beta + \sum_{k=1}^{N-1} X_{k+1,n}(W_{1,2k+1} - W_{2,2k+2})\right]^2 + \left(\nu_1 + X_{8,n}\nu_2 + \sum_{k=1}^{N-2} X_{k+1,n}W_{1,2k+2}\right)\left(\nu_1 + X_{2,n}\nu_2 + \sum_{k=1}^{N-2} X_{k+2,n}W_{2,2k+3}\right)\right\}^{1/2} \quad (4)$$

The coefficients, X, are complex numbers determined by

$$X_{k,n} = \exp\left[i\frac{2\pi}{N}n(k-1)\right] \quad (5)$$

Following the published approach (*36*), the excitonic manifold is determined via a semiempirical INDO/S calculation using truncated BChl molecules positioned according to a symmetrized set of coordinates from the *Rsp. molischianum* LH2 structure. The resulting manifold contained four nondegenerate levels, corresponding to the levels where $n = 4$ and $n = 8$. These four levels were used to fit four parameters: ε, the site energy of the BChls (only a single value since the assumption of $\varepsilon = \varepsilon_\alpha = \varepsilon_\beta$ was used), ν_1, ν_2, and $W_{1,3}$. The last parameter allows the calculation of the value of C by

$$C = W_{1,3}\left[\frac{d_1 \cdot d_3}{|R_{1,3}|^3} - \frac{3(d_1 \cdot R_{1,3})(d_3 \cdot R_{1,3})}{|R_{1,3}|^5}\right]^{-1} \quad (6)$$

where the vector parameters are provided by the symmetrized set of coordinates. The resulting fitted values were $\varepsilon = 13362\ cm^{-1}$, $\nu_1 = 806\ cm^{-1}$, $\nu_2 = 377\ cm^{-1}$, and $W_{1,3} = -152\ cm^{-1}$, which gives a value of $C = 519310\ Å^3\ cm^{-1}$.

Using these values, the equation for the Q_y transition is composed of two degenerate states corresponding to the (−) form of the equation when $n = 1$ and $n = N - 1$. For this analysis, an assumption is made that the mutations introduced alter only the site energies of the BChls, leaving the geometry and coupling interactions untouched. With this assumption, many of the terms in eq 4 can therefore be grouped together. For use in an equation describing the Q_y transition for a symmetrical LH complex, three parameters are defined that are taken to be constant for a given LH complex:

$$\sigma_1 = \sum_{k=1}^{N-1} X_{k+1,1}(W_{1,2k+1} + W_{2,2k+2}) \quad (7)$$

$$\sigma_2 = \sum_{k=1}^{N-1} X_{k+1,1}(W_{1,2k+1} - W_{2,2k+2}) \quad (8)$$

$$\sigma_3 = \left(\nu_1 + X_{8,1}\nu_2 + \sum_{k=1}^{N-2} X_{k+1,1}W_{1,2k+2}\right)\left(\nu_1 + X_{2,1}\nu_2 + \sum_{k=1}^{N-2} X_{k+2,1}W_{2,2k+3}\right) \quad (9)$$

The energy for the Q_y transition, E_{Q_y} (eq 4), can then be written in terms of the site energies, ε_α and ε_β, as

$$E_{Q_y} = \frac{\varepsilon_\alpha + \varepsilon_\beta}{2} + \frac{1}{2}\sigma_1 - \left\{\frac{1}{4}(\delta\varepsilon + \sigma_2)^2 + \sigma_3\right\}^{1/2} \quad (10)$$

where $\delta\varepsilon = \varepsilon_\alpha - \varepsilon_\beta$. For LH2 from *Rps. acidophila* and *Rb. sphaeroides*, the values for these constants are $\sigma_1 = -348.202$, $\sigma_2 = -63.6535$, $\sigma_3 = 1317709$, and for the LH1 complex, these constants are $\sigma_1 = -499.874$, $\sigma_2 = -1.184187$, $\sigma_3 = 1517107$ (all values are in cm^{-1}).

RESULTS

The optical absorption spectra of the mutants all have a single absorption band in the near-infrared region of 855−880 nm with different positions for the peak maximum, λ_{max} (Figure 2). In general, mutations at the wild-type hydrogen bond donor positions α43 and β48 have a more significant effect on λ_{max} than mutations at residue α44. The observed spectra of the mutants have line widths comparable to previous measurements at room temperature, noting that low-temperature measurements of LH1 show a significant decrease (*38*).

The wild type and five mutants with the native Trp α43 hydrogen bond donor have the largest λ_{max}, ranging from 879 nm for wild type (WLW) to 868 nm for the WFF mutant. Of these five mutants, the two with the native Trp β48, WYW and WFW, are the most similar to wild type with λ_{max} values of 875 and 874 nm, respectively. The three other mutants that have Phe at β48, WLF, WYF, and WFF, have absorption band positions that are shifted further to the blue with λ_{max} at 872, 870, and 868 nm, respectively. The two mutants with the hydrogen bond from Trp α43 not present due to the substitution of this residue with Phe, FYW and FLW, have the most shifted bands with λ_{max} at 867 and 856 nm, respectively. The shifts for the WLF and FLW mutants agree with previous measurements (*21*, *22*). The mutations at the α44 position result in relatively small but consistent perturbations of the spectra compared to the larger changes

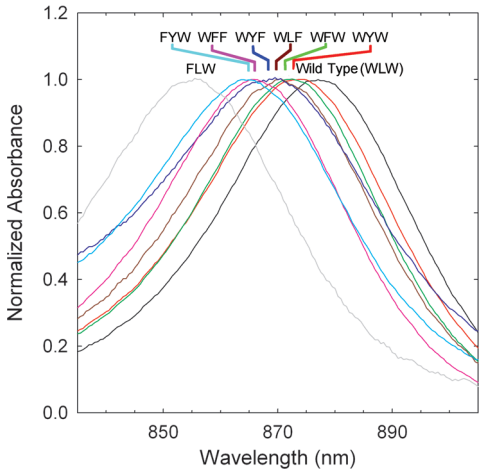

FIGURE 2: Normalized absorption spectra of isolated wild-type and mutant LH1 complexes measured at 8 °C. The peak position (λ_{max}) is at 879 nm in the wild type (WLW, Trp α43, Leu α44, Trp β48), 875 nm in the WYW mutant (Leu α44 to Tyr), 874 nm in the WFW mutant (Leu α44 to Phe), 872 nm in the WLF mutant (Trp β48 to Phe), 870 nm in the WYF mutant (Leu α44 to Tyr and Trp β48 to Phe), 868 nm in the WFF mutant (Leu α44 to Phe and Trp β48 to Phe), 867 nm in the FYW mutant (Trp α43 to Phe and Leu α44 to Tyr), and 856 nm for the FLW mutant (Trp α43 to Phe).

imposed by altering Trp α43. They produce a consistent relationship of decreasing λ_{max} with the largest shifts from the Leu substitution and Tyr and Phe resulting in smaller shifts.

These optical measurements were performed using the detergent lithium dodecyl sulfate based upon a previously developed protocol that had been shown not to shift the optical spectrum or resonance Raman compared to the membrane spectrum (*34*, *38*). As with any detergent, use of certain conditions can disrupt the membrane protein complex as found for LH1 when isolated using the combination of a high concentration of lithium dodecyl sulfate with polyacrylamide gel electrophoresis (*39*, *40*). While the detergent concentration was maintained at 0.05% for most experiments on the LH1 mutants, measurements using concentrations up to 0.1% showed no changes in the optical spectra. Even when the isolated complexes were at 22 °C for a short period of time rather than 8 °C, no shifts to shorter wavelengths were observed as would be expected if fragmentation was occurring. To ensure against any possible unexpected effects due to the use of lithium dodecyl sulfate, complexes were isolated from the membranes for all of the mutants using the detergent octyl β-glucoside. For all cases, the experimental optical spectrum matched for the two detergents (data not shown). In addition, the spectral shifts reported here for the purified complexes of the mutants compared to wild type are the same as previously reported for the shifts seen in chromatophores of the WLF and FLW mutants compared to wild type (*21*, *22*).

The intactness of the complex after detergent extraction was investigated by measurement of the size of the LH1 preparations using size-exclusion chromatography. These results showed that the samples contained only one, very large, complex with an estimated molecular mass of 210 ± 30 kDa, consistent with the estimated molecular mass of 220 kDa. The presence of a complex with a low molecular weight, for example, a complex consisting of only two protein subunits, was not detected. In these experiments, the complexes derived from the mutant strains behaved identically to wild type.

The resonance Raman spectra for the seven mutants show distinctive changes compared to the wild-type complex (Figure 3).

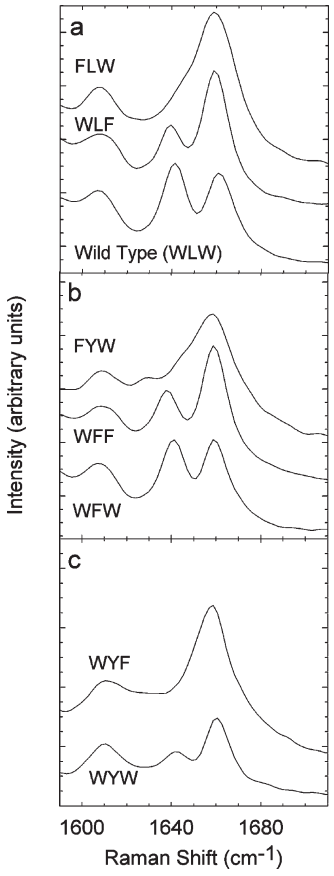

FIGURE 3: Fourier-transform resonance Raman spectra for wild-type and mutant LH1 complexes: (a) wild type, FLW, and WLF mutants that have been previously reported in the literature (*21*, *24*); (b) the WFW, WFF, and FYW mutants; (c) the WYF and WYW mutants. The mutants are named according to the identity of the residue at positions α43, α44, and β48, which in wild type (WLW) are Trp α43, Leu α44, and Trp β48.

The spectrum of the purified wild-type LH1 has three peaks at 1607, 1641, and 1661 cm^{-1} in agreement with previous studies of wild type in membrane fragments (*22*). The peak at 1607 cm^{-1} has been assigned to a coordination-sensitive methine bridge-stretching mode, and the peaks at 1641 and 1661 cm^{-1} have been assigned to the hydrogen-bonded C3-acetyl groups and the C13-keto groups, respectively. The spectrum of the WLF mutant, with the single change of Trp β48 to Phe, shows a shift of intensity from the region near 1641 cm^{-1} to the region near 1660 cm^{-1}, indicating the loss of one of the hydrogen bonds (*21*). The signal from the remaining hydrogen-bonded acetyl group is clearly visible at 1639 cm^{-1}. The spectrum of the FLW mutant with the single change of Trp α43 to Phe has a shift of intensity from the band at 1641 cm^{-1} to the band near 1660 cm^{-1} and is consistent with the loss of the hydrogen bond as previously reported for this mutant in membrane fragments (*22*). The signal from the remaining hydrogen-bonded acetyl group is poorly resolved from the 1660 cm^{-1} band but can be seen as a shoulder to this band near 1642 cm^{-1}. Taken together with the model of the *Rsp. molischianum* LH2 structure, the interpretation of these spectra of the purified complexes is that the mutation of Trp α43 to Phe removes the hydrogen bond to the α-bound BChl, leaving the hydrogen bond to the β-bound BChl unchanged, while the mutation of Trp β48 to Phe removes the hydrogen bond to the β-bound BChl, leaving the hydrogen bond to the α-bound BChl unchanged as previously concluded based upon measurements of the cell membranes (*21*).

The change of Leu α44 to Phe in the WFW mutant results in a spectrum that is nearly identical to wild type with the acetyl group peak at 1641 cm^{-1} and the keto group peak slightly shifted to 1659 cm^{-1}. The WFF mutant, which combines this mutation with the Trp β48 to Phe mutation, results in a spectrum that is nearly identical to the WLF spectrum with peaks at 1638 and 1659 cm^{-1} and the methine peak shifted slightly to 1609 cm^{-1}. In both cases, it appears that replacement of Leu α44 with Phe does not disturb the hydrogen bond arrangement. The spectrum of the FYW mutant, which has both Trp α43 and Leu α44 changed, is different from the spectra described so far but is the most similar to that of the FLW mutant. In the spectrum of the FYW mutant, the largest peak is near 1659 cm^{-1}, but it is smaller than the one in the FLW spectrum. The spectrum has a poorly resolved shoulder near 1642 cm^{-1} as in the FLW spectrum, but it also has a new peak at 1630 cm^{-1}. The spectrum also shows a small shift of the methine peak to 1609 cm^{-1}. This spectrum of the purified FYW mutant is very similar to the one reported for a mutant that has Trp α43 replaced with Tyr (*22*) and likely represents the case where a hydrogen bond is now being donated by Tyr α44.

The remaining two mutants, the WYW and WYF mutants, both have Tyr α44 and result in rather distinctive spectra. Although the WYW mutant has the two wild-type hydrogen bond donors, Trp α43 and Trp β48, at first glance its resonance Raman spectrum appears similar to the spectra of the mutants lacking the hydrogen bond from Trp β48, namely, the WLF and WFF mutants. The peak at 1661 cm^{-1} is the largest in the spectrum and is greater than twice the intensity of the signal at 1641 cm^{-1}. The spectrum for the WYW mutant does have some significant differences with the spectra of the two β48 mutants, WLF and WYF. The peak for the methine bridge stretching shifts to 1611 cm^{-1}, and the relative size of the 1661 cm^{-1} peak compared to the 1611 cm^{-1} peak is more similar to that of the ones in spectra with both native hydrogen bond donors, the wild type and WFW mutant. Additionally, the peak near 1640 cm^{-1} is actually at 1641 cm^{-1}, indicating that it has contributions from both the signal at 1639 cm^{-1}, the one for the hydrogen-bonded α-bound BChl, and the signal at 1642 cm^{-1}, the one for the hydrogen-bonded β-bound BChl. It appears that the result of replacing Leu α44 with Tyr is a partial loss of the intensity at 1639 cm^{-1} but no apparent gain of intensity at 1660 cm^{-1}. The WYF mutant has a spectrum that appears to show no hydrogen-bonded C3-acetyl groups as the only peaks are at 1611 and 1659 cm^{-1}. However, a close examination of the spectra of the WYW and WYF mutants shows a broad and weak signal in the region between 1620 and 1640 cm^{-1}, and this signal likely contributes to the apparent shift of the methine peak in the spectra of these mutants.

DISCUSSION

Eight LH1 complexes were examined in this study, including the wild type, which has residues Trp α43, Leu α44, and Trp β48 (designated WLW), and seven mutants with single or double changes at these residues. Four of these mutants have changes solely in the α-peptide at α43 or α44: FLW, WFW, FYW, and WYW. The FLW mutant, with the change of the hydrogen bond donor Trp α43 to Phe, has been thoroughly discussed in the literature (*21*, *22*). Of principal relevance to these results is the conclusion that only part of the large blue shift observed in the absorption spectrum of this mutant, with respect to wild type, could be attributed to the loss of a hydrogen bond. The remainder of the shift was attributed to some other cause, such as a structural change that alters the excitonic interactions in the complex. The WFW mutant, with the change Leu α44 to Phe, provides an example of a complex where a significant shift, 5 nm to the blue, can be accomplished while leaving the hydrogen-bonding arrangement undisturbed. The observed shift is assumed to arise from structural differences between this mutant complex and the wild type, but in the absence of structural data, assigning the specific type of structural difference is difficult.

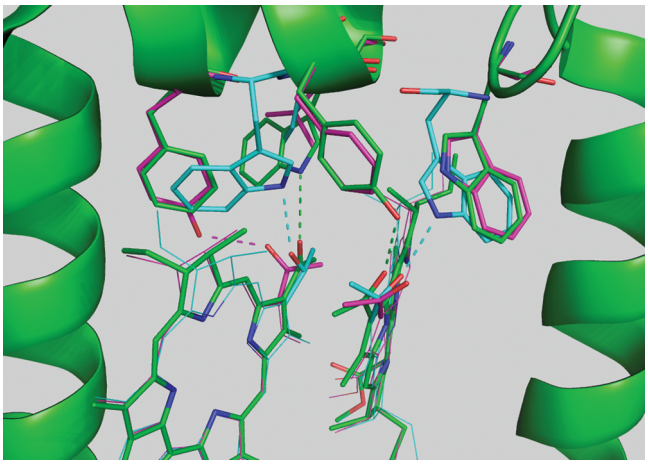

FIGURE 4: Superposition of the structures of the *Rsp. molischianum* LH2 complex (cyan) and the *Rps. acidophila* LH2 (green) and LH3 (magenta) complexes showing the hydrogen bonding to the C3-acetyl groups of the excitonically coupled BChls. In the *Rsp. molischianum* LH2 complex, hydrogen bonds are provided by residues Trp α45 and Trp β48. In the *Rps. acidophila* LH2 complex, hydrogen bonds are provided by residues Tyr α44 and Trp α45, and in the LH3 complex a hydrogen bond is provided by Tyr α41. In the *Rb. sphaeroides* LH2 complex, the hydrogen-bonding pattern is believed to be similar to that observed for the *Rps. acidophila* LH2 complex with the analogous residues Tyr α44 and Tyr α45. In the *Rb. sphaeroides* LH1 complex, the hydrogen-bonding pattern is believed to be similar to that observed for the *Rps. molischianum* LH2 complex with the analogous residues Trp α43 and Trp β48. In this picture, the *Rs. molischianum* LH2 Ile α46 occupies the same region as *Rps. acidophila* LH2 Trp α45. The analogous residue in the *Rb. sphaeroides* LH1 complex is Leu α44.

The FYW double mutant (Trp α43 to Phe and Leu α44 to Tyr) is very similar to the previously reported mutant in which Trp α43 was altered to Tyr (*22*). The differences between the Raman spectra of the FLW and FYW mutants point to the formation of a hydrogen bond in the latter mutant, presumably from Tyr α44. The previously reported similarity between the LH1 complex and the LH2 complex from *Rsp. molischianum* (*20*) provides a model by which the feasibility of this arrangement can be assessed. In the three-dimensional structure of LH2 from *Rsp. molischianum*, the acetyl groups for the α- and β-bound BChls are hydrogen bonded to Trp residues at α45 and β44, respectively (*9*). The analogous residues in the LH1 complex of *Rb. sphaeroides* are Trp residues at α43 and β48. The hydrogen bond donors in the LH2 complex of *Rps. acidophila* are Tyr α44 and Trp α45. An overlay of the LH2 and LH3 complexes from *Rps. acidophila* and the LH2 complex from *Rsp. molischianum* shows a close match of the B850 BChls (Figure 4). Trp α45 from the *Rps. acidophila* LH2 structure can be seen to occupy the same region of space as Ile α46, which is one residue past the hydrogen bond donating Trp α45, in the *Rsp. molischianum* LH2 structure. As a result, there appears to be the capability for a residue in this region to form a hydrogen bond with the α-bound BChl. If Ile α46 in this structure

Table 1: Experimental and Calculated Absorbance Maxima for Solubilized LH1 Complexes

strain[a]	ΔE contributions[b]	ΔE (cm^{-1})	$\Delta\lambda_{calc}$ (nm)	$\Delta\lambda_{obs}$ (nm)[c]
WLW (wild type)				
WYW	ΔE_S(LYα44)	39.2	3	4
WFW	ΔE_S(LFα44)	59.0	4.5	5
WLF	ΔE_S(WFβ48) + ΔE_H	78.7	7	7
WYF	ΔE_S(LYα44) + ΔE_S(WFβ48) + ΔE_H	117.9	9	9
WFF	ΔE_S(LFα44) + ΔE_S(WFβ48) + ΔE_H	137.7	10.5	11
FYW	ΔE_S(WFα43) + ΔE_S(LYα44)	151.2	11.5	12
FLW	ΔE_S(WFα43) + ΔE_H	299.4	22.5	23

[a]Mutants are named according to the identity of the residue at positions α43, α44, and β48; for example, wild type (Trp α43, Leu α44, Trp β48) is named WLW, and the mutant with the single mutation Trp α43 to Phe is named FLW. [b]Contributions to the change in the Q_y transition energy as fitted using eq 11 and the values ΔE_S(LYα44) = 39.2 cm^{-1}, ΔE_S(LFα44) = 59.0 cm^{-1}, ΔE_S(WFβ48) = −108.8 cm^{-1}, ΔE_S(WFα43) = 112.0 cm^{-1}, and ΔE_H = 187.4 cm^{-1}, where the structural term LYα44 is for the change Leu α44 to Tyr, LFα44 is for the change Leu α44 to Phe, WFβ48 is for the change Trp β48 to Phe, and WFα43 is for the change Trp α43 to Phe. [c]Experimental shift of the absorption peak compared to the 879 nm band of wild type.

is replaced by Tyr, alteration of neither the backbone nor the dihedral angle positioning the side chain is necessary to allow the tyrosyl oxygen to be positioned within hydrogen-bonding distance of the C3-acetyl group. If a similar arrangement exists in the LH1 complex of *Rb. sphaeroides*, it seems reasonable to expect that Tyr at α44 could form a hydrogen bond with the acetyl group of the α-bound BChl.

The potential of Tyr α44 to form a hydrogen bond to the same C3-acetyl group as Trp α43 presents the possibility of two hydrogen bonds to the α-bound BChl when both of these residues are present, as in the WYW (Trp α43, Tyr α44, Trp β48) and WYF (Trp α43, Tyr α44, Phe β48) mutants. In the resonance Raman spectrum of the WYW mutant, there appears to have been a loss of intensity near 1641 cm^{-1} but no corresponding gain in intensity near 1660 cm^{-1}. Such a spectrum may arise from a BChl conformation where the C3-acetyl group has rotated so far out of the plane of the macrocycle that it no longer experiences the resonance enhancement effect. However, when taken in conjunction with the ability of Tyr α44 to form a hydrogen bond to the same C3-acetyl group as Trp α43, the picture that arises is one in which there is a competition between these two residues for the same C3-acetyl group in the WYW and WYF mutants, in which either Trp α43 or Trp α44 forms a hydrogen bond but not both simultaneously. The broad, weak intensity observed for both of these mutants in the 1620−1640 cm^{-1} region is likely the result of some combination of the 1629 cm^{-1} signal observed in the FYW mutant and the 1639 cm^{-1} signal observed in the WLF mutant. The WYW spectrum is therefore interpreted as representing two hydrogen bonds, in which each individual mutant has one hydrogen bond from Trp β48 and one hydrogen bond from either Trp α43 or Trp α44, while the WYF spectrum corresponds to each mutant having a single hydrogen bond, from either Trp α43 or Trp α44.

The mutation of Trp β48 to Phe removes the wild-type hydrogen bond donor. A 6 nm blue shift has previously been reported as being the result of the loss of the hydrogen bond to the C3-acetyl group of the β-bound BChl in this single mutant (*21*). In this study, this mutation has been performed in conjunction with the mutations to the α-peptide described above. The Raman spectra (Figure 3) show the distinct loss of a hydrogen bond when comparing mutants whose sole difference is at β48. For example, when comparing wild type (WLW) and WLF or comparing WFW and WFF, a shift in intensity from the 1641 cm^{-1} region to the 1660 cm^{-1} region is evident, indicating the loss of the hydrogen bond to the β-bound BChl. Comparison of the optical spectra (Table 1) shows that, independent of the identity of the residue at position α44, alteration of β48 produces similar shifts of approximately 6 nm. Likewise, independent of the residue at position β48, alteration of the residue at position α44 produces comparable shifts of 4−5 nm. The mutations at either position α44 or position β48 appear to produce changes that are largely conservative and independent of one another. In addition to the changes being independent of one another, the effects that result from single mutations seem to be additive when two mutations are performed together. For example, the difference of 11 nm between wild type (WLW) and WFF (Leu α44 to Phe and Trp α43 to Phe) is very close to the sum of the 5 and 7 nm shifts observed for the individual mutants WFW (Leu α44 to Phe) and WLF (Trp α43 to Phe), respectively. These differences hold not only for each mutant compared to wild type but also when comparing two mutants. A similar pattern is also seen in the *Rb. sphaeroides* LH2 mutants (*24*, *25*). This type of pattern of independent and additive shifts is consistent with a situation in which the individual α and β mutations alter only the individual site energies of the α- and β-bound BChls.

The structure of the LH3 complex raises the possibility that the changes in the absorption spectra observed here and in previous work are at least partly due to structural changes and not solely the result of the removal of hydrogen bonds. The consistency of the shifts observed when altering the hydrogen bonding to the monomeric BChl in LH2 and the coupled BChls in LH1 and LH2 implies a significant effect for hydrogen bonding on the electronic structure. Previous mutagenesis work on LH1 invoked the possibility of a structural change to explain the large shift on mutating Trp α43 to Phe, which removed a hydrogen bond, as well as the difference observed on mutating Trp α43 to Tyr (*22*), which did not remove the hydrogen bond. Likewise, the difference between the absorption spectra of wild type (WLW) and WFW (with the change Leu α44 to Phe) requires some cause other than hydrogen bonding, as their resonance Raman spectra are nearly identical. It is therefore likely that the mutations reported here and in the literature induce shifts in the absorption spectra that are not due solely to the alteration of the hydrogen bonding of the pigments. However, in the absence of structural data, it is difficult to determine the relative contributions that structural and hydrogen-bonding changes make to these observed shifts. One approach is to alter the complex while maintaining the hydrogen bonds to the acetyl groups. In this case, the spectral difference between the mutant and wild type would be due solely to structural alterations.

Differentiating the Effects of Hydrogen-Bonding and Structural Changes. Comparison of the properties of the

mutants allows an estimation of the effect of structural changes that accompany the mutations. In particular, the combination of the hydrogen-bonding ability of Tyr α44 with the alteration of Trp α43 to Phe in the FYW mutant yields the same number of hydrogen bonds in the mutant as the wild type (WLW). If the structural changes that accompany the replacement of Trp α43 with Phe are independent of other changes, then the difference between the FYW and WYW mutants provides an estimation of the structural contribution to the spectral difference between the FLW mutant and the wild type (WLW). This in turn should allow an estimation of the change in absorption spectra due solely to the hydrogen bonding of the C3-acetyl groups. This analysis follows the approach of Olsen and co-workers (*22*), who examined the optical differences between wild type, the Trp α43 to Tyr mutant, and the Trp α43 to Phe mutant. The structural similarity of the Tyr and Phe residues provoked the possibility that similar structurally dependent shifts were occurring in the two mutants and that the most representative value for the effect of the loss of a hydrogen bond could be seen in the difference between the two mutants, as opposed to the difference between the mutant and wild-type complexes. Here we take this approach and apply it to the differences observed between the LH complexes described in this paper.

It is assumed that the difference between the observed Q_y transition energies, $\Delta E_{Q_y}(A/B)$, of two LH complexes, A and B, can be partitioned into a structural and a hydrogen bond component:

$$\Delta E_{Q_y}(A/B) = E_{Q_y}(B) - E_{Q_y}(A) = \Delta E_S(A/B) + \Delta E_H \quad (11)$$

where $\Delta E_S(A/B)$ is the change in the transition energy due solely to structural differences between the two complexes and ΔE_H is the change in transition energy due to any changes in hydrogen bonding to the C3-acetyl groups. For the set of mutants in this paper, there are four parameters, one for the Trp α43 to Phe mutation, one for the Trp β48 to Phe mutation, and two for the change of Leu α44 to Phe and Tyr. If the number of hydrogen-bonded C3-acetyl groups is the same in complexes A and B, then ΔE_H is set equal to zero, and any difference between the observed transition energies is interpreted as being due solely to structural differences.

For the eight LH1 complexes presented in this paper, there are 28 unique pairing combinations. The Solver tool in Excel was used to adjust the fitted values of the four structural parameters and one hydrogen bond parameter to yield the lowest sum of the squared deviations for the 28 equations. The resulting values of the five parameters are 39.2 cm^{-1} for ΔE_S(LYα44), corresponding to the Leu α44 to Tyr mutation, 59.0 cm^{-1} for ΔE_S(LFα44), corresponding to the Leu α44 to Phe mutation, −108.7 cm^{-1} for ΔE_S(WFβ48), corresponding to the Trp β48 to Phe mutation, 112.0 cm^{-1} for ΔE_S(WFα43), corresponding to the Trp α43 to Phe mutation, and 187.4 cm^{-1} for ΔE_H. When the fitted parameters are used to calculate the shifts of the peak wavelength positions of the seven mutants relative to wild type, the resulting differences are within 1 nm of the experimentally determined values (Table 1).

The parameters with the smallest values, 39.2 and 59.0 cm^{-1}, are for the insertion of Tyr or Phe for Leu α44, respectively. These parameters reflect the relatively small spectral shifts for those mutants and the limited impact that the Leu substitution has on the three-dimensional structure even when Tyr, which is much bulkier, is substituted in the hydrogen-bonded position. In contrast, substitution of Trp by Phe, which might be considered to be a much more conservative change, at either β48 or α43 results in much larger contributions of −108.7 and 112.0 cm^{-1}, respectively. The negative sign for the β48 substitution represents a shift to longer wavelengths. However, all mutants show a shift to shorter wavelengths as the β48 substitution also results in a loss of a hydrogen bond resulting in a net positive change in energy (Table 1). The possible reasons for the opposite shifts are discussed below. The largest contribution, a value of 187.4 cm^{-1} for ΔE_H, is found to arise from the effect of hydrogen bonding. This value is in general agreement with the contribution of changes in hydrogen bonds estimated from other mutagenesis studies of LH1. Previously, the mutation of Trp α43 to Tyr and Phe has been shown to result in blue shifts of 12 and 24 nm, respectively (*21*, *22*).

Interpreting the Structural Contributions. The approach described in the previous section interpreted the spectral differences among the various LH1 complexes in terms of structural and hydrogen bond parameters without regard for what these structural changes are or how they specifically affect the excitation energy of the complex. The pattern of spectral changes that occur with mutations of both the LH1 and LH2 complexes points to a situation where individual mutations alter the site energies of either the α- or β-bound BChls, regardless of whether the effect of the mutation is interpreted as being due to a structural or hydrogen bonding change. As a result, the type of structural changes that accompany the mutations described in this paper, whether they alter the hydrogen bonding to the acetyl groups or not, may alter only the site energy of the BChls and not the excitonic coupling between them. Changes arising from the alteration of hydrogen bonding are well-defined in terms of the observed spectral changes of the absorption and resonance Raman spectra. Effects due to some of the other changes cannot be excluded, and so the interpretation should be regarded as representing an upper limit for the effects due to hydrogen bonding. Thus, the data will primarily be used to establish whether the observed spectral changes can be interpreted in terms of changes in hydrogen bonding and subsequent rotations of the acetyl groups.

The Q_y transition energy can be expressed in terms of the site energies for the α- and β-bound BChls and the summations of several of the dipolar coupling terms for the pigments in the LH complex, assuming that the mutations being examined do not appreciably alter the positions or orientation of the BChl pigments (eq 10). For the evaluation of mutations that alter only one of the site energy values, the difference in the observed energy of the Q_y transition, ΔE_{Q_y}, as the function of a change in the site energy of either the α- or β-bound BChl, $\Delta\varepsilon_{\alpha/\beta}$, is found to be

$$\Delta E_{Q_y} = \frac{\Delta\varepsilon_{\alpha/\beta}}{2} - \left[\frac{1}{4}(\delta\varepsilon \pm \Delta\varepsilon_{\alpha/\beta} + \sigma_2)^2 + \sigma_3\right]^{1/2} + \left[\frac{1}{4}(\delta\varepsilon + \sigma_2)^2 + \sigma_3\right]^{1/2} \quad (12)$$

The (+) form of the equation is used for changes to α site energies while the (−) form of the equation is used for changes to the β site energies. The value of σ_3 is dramatically larger than any of the other parameters so the first square root term largely cancels out the second square root term. As a result, if only one of the site energies changes, then the change in the transition energy is

approximately half of the change in the site energy:

$$\Delta E_{Q_y} \approx \Delta\varepsilon/2 \quad (13)$$

Using this approximation, the pattern of independent and additive shifts observed for the Q_y transitions of the mutant LH1 complexes can be linked to changes in the individual site energies of the BChl pigments.

One critical parameter that could result in a shift of the Q_y transition is a rotation of the acetyl group of a BChl. The dependence of the site energy of a BChl can be expressed in terms of the acetyl group angle, ω, using the empirical relationship:

$$\varepsilon(\omega) = \varepsilon(0) + \rho\omega + b_H\left(1 - \frac{\omega}{90°}\right) \quad (14)$$

where $\varepsilon(0)$ is the site energy of the molecule with the acetyl group completely in plane and lacking a hydrogen bond, ρ is a scaling parameter, and ω is defined as the dihedral angle for the acetyl group by C2B−C3B−CAB−OBB that equals zero when the acetyl group is in plane. The second term approximates a previously described dihedral dependence (*29*). A value of 8 cm^{-1}/deg is assigned to ρ based upon an estimate of 320 cm^{-1} for a 40° angle (*41*). The parameter b_H is the effect of a hydrogen bond when the acetyl group is completely in plane ($\omega = 0$) and is zero if no hydrogen bond is present. Based upon He and coworkers (*42*), this term has a value of 364 cm^{-1} for the loss of a hydrogen bond to an acetyl group with a dihedral angle of 30°, yielding a b_H value of 546 cm^{-1}. The usefulness of these empirical dependences is evident when relating the Q_y transition energies to the observed torsion angles for the BChl in the FMO protein that contains seven BChls whose conformations have been determined at high resolution (*29*, *43*−*45*).

The opposite signs of ΔE_S for the β48 and α43 mutants, having values of −108.8 and +112.0 cm^{-1}, respectively, may be explained in terms of the rotation of the acetyl group. Assuming that the structural difference is due to changes in the angle of the acetyl group, the opposite signs represent opposite rotations of this group relative to wild type. Using the approximation that the shift of the energy of the Q_y transition energy is half of the site energy change (eq 13), the structural change for the α43 mutation may be modeled as a 15° rotation of the acetyl group away from the BChl plane while the β48 mutation would arise from a comparable rotation but in the opposite direction, namely, toward the BChl plane. In contrast, the small structural components of 39.2 and 59.0 cm^{-1} for the insertion of Tyr or Phe for Leu α44, respectively, suggest that the acetyl groups have angles similar to wild type in these two mutants.

The protein surrounding the BChls may influence the absorption spectrum of the LH1 complex in different ways, including providing side chains that directly interact with the tetrapyrroles, through dispersive forces, or steric hindrance (*4*, *46*). The hydrogen-bonding state has been shown in a number of different experiments involving LH1 and LH2 to strongly affect the spectrum. For example, in LH2 when Tyr α44 and Trp α45, which are involved in hydrogen-bonding interactions with the BChls, are replaced by phenylalanine and leucine, the peak wavelength is decreased from 850 to 826 nm (*23*). Similar changes in the absorption spectrum are measured for the corresponding mutations reported here for LH1. These effects can be understood in terms of changes in the site energies of the individual BChls that affect the excitonically coupled levels of the collective system. Associated with the change in hydrogen bonding is a potential rotation of the acetyl group that has been modeled to result in a shift of the optical spectrum (*27*, *29*, *41*, *47*, *48*). A shift to higher energy is expected for rotation of the acetyl group completely out of plane in terms of effectively lowering the extent of conjugation in the system and also by analogy to BChl derivatives that have the acetyl group converted to a hydroxyl group (*49*). Another possible interaction that could influence the spectrum is hydrogen bonding to the keto group of the BChl. However, it has been shown in both LH1 and LH2 that breaking of this interaction through mutagenesis does not alter the Q_y transition (*50*, *51*). The lack of influence of this interaction probably is because this group is less conjugated with the macrocycle.

The conformation of the macrocycle may play a role in tuning the spectrum based upon isolated porphyrin models in solvent (*29*, *52*). Steric hindrance from side groups can lead to features such as ruffling or saddling, resulting in large spectral shifts and decreases in the lifetime of the first excited singlet state. The LH2 complex shows that the β-bound BChl can have a distorted tetrapyrrole and the different BChls exhibit different conformations in the three-dimensional structures (*53*, *54*). However, even at the best resolution of 2.0 Å, the errors of the positions of the BChl atoms are still approximately 0.2−0.3 Å and dependent upon the specific library used in the refinement. The distortions of the BChls in LH2 that are observed are also much smaller than those seen in synthetic systems, and the contribution of these distortions to the BChl site energies is unclear. Due to the lack of a high-resolution structure, there is no structural evidence of such distortion for the BChls in LH1. Spectroscopic studies have established a distortion of the BChls of LH1 and LH2 compared to the relaxed conformation of the isolated pigments in organic solvents, but such features are the same when comparing the spectra of mutants or the LH1 and LH2 complexes from different species (*55*).

The estimates of the alterations of the site energies of the individual BChls use the assumption of a symmetrical arrangement of the proteins forming the LH1 complex. However, a number of experiments show that while this assumption is a fair approximation, LH1 does not have this precise symmetry. The reaction center−LH1 complex has been visualized by electron microscopy and found to form regular hexagonal arrays in *Bl. viridis* (*56*). The LH1 complex from *Rsp. rubrum* reconstituted from the individual proteins shows a circular arrangement with 16 pairs of protein subunits with the center empty (*11*). More recently, a variety of arrangements have been reported, including circular (*57*), square (*58*), and open arcs (*17*), with some arrays showing a 2-fold symmetry involving two interacting LH1 complexes (*18*, *59*) that are more symmetrical in the absence of the reaction center.

A number of experiments have shown that disorder plays a critical role in defining the functional properties of the LH complexes. For example, the position of the fluorescence electronic transition is dependent upon the wavelength of the excitation at low temperatures, suggesting a mixture of populations of the LH complex due to either a static or dynamical disorder (*60*). The otherwise identical BChls have different electronic states because of such disorder. The disorder could have a major impact on the distribution of the electronic states over the BChls, in particular any localization of the excitation energy. Modeling of disorder as giving rise to fluorescence properties of the LH complexes at low

temperatures shows the pigments to be highly coupled with the disorder large enough to disrupt the delocalization of the excited states. While absorption and circular dichroism spectroscopy would be useful in determining the parameters of these models, interpretation of the spectrum of the LH1 complex has proven to be difficult, as the almost identical arrangement of the transition dipoles in the plane of the rings causes the contributions to nearly cancel, making the signal sensitive to small variations due to local disorder (*61*).

The impact of such effects can be modeled in terms of the Hamiltonian (eq 1). The assumption of symmetry allows the electronic states to be considered as being delocalized over the N equivalent pigments. However, the symmetry can broken by different effects on the BChls (*4*, *46*). Local variations in the protein environment of the binding sites result in a static disorder in the site energies of the pigments that alters the diagonal elements of the Hamiltonian. Deviations from perfect symmetry give rise to a variation in the pigment−pigment interactions that affect the off-diagonal elements. Dynamics such as low-frequency oscillations of the protein lead to a time-dependent variation in the site energies and interactions of the pigments. In principle, such factors can be calculated using high-resolution structures, but it remains a challenge to perform such calculations, even for the highly symmetrical LH2 complex. These terms for LH2 show a wide range of values; for example, the interaction strength of the pigments has been estimated to be 240−770 cm^{-1}. The structural variations, namely, the ellipticity of the LH1 ring or interruption of the ring due to the presence of PufX, are expected to be minor compared to the impact of disorder on the Hamiltonian parameters. Detailed studies show only a very minor change of 1−2 nm in the peak position of the Q_y transition of the optical spectrum, and single-molecule spectroscopic measurements suggest that such disorder has little impact on the exciton manifold when comparing strains with and without the PufX protein (*62*, *63*). Such small shifts are comparable to what is observed due to changes in the growth conditions. The disorder of the LH2 complex is large enough to affect the delocalization of the exciton over the coupled BChls as shown by the fluorescence properties and other spectroscopic measurements (*4*, *46*). For LH1, disorder can arise from differences in the arrangement of the ring or the involvement of the PufX protein. Solvation effects, which could influence the vibrational states of the BChls, have been shown to systematically shift the optical spectrum, although only at very high, non-natural pressures (*64*−*66*), suggesting that their involvement at ambient pressures is limited.

Comparison of the Structural and Hydrogen Bond Effects on Different LH Complexes. These models developed for the LH1 complex can be extended to the LH2 and LH3 complexes. The dihedral angles for the α- and β-bound BChls are 14° and 24° for LH2 and 48° and 45° for LH3 of *Rps. acidophila* (*10*), and the effective parameters are $\sigma_1 = -348.2$ cm^{-1}, $\sigma_2 = -63.6$ cm^{-1}, $\sigma_3 = 1317800$ cm^{-1}, with $b_H = 546$ cm^{-1} and $\rho = 8$ cm^{-1}. For wild-type LH2, the values of ε_α and ε_β are approximated as being equal, to give the experimentally observed value for the Q_y transition, and calculated to be 12963 cm^{-1}. For LH3, the two values are slightly different at 13441 and 13531 cm^{-1} for ε_α and ε_β, respectively. The transition energy for LH3 is calculated to be 520 cm^{-1} larger than LH2 in agreement with the observed 584 cm^{-1} value or, equivalently a calculated peak of 822 nm rather than the observed 818 nm. The difference is seen as arising from roughly equivalent contributions from acetyl rotations, the loss of the hydrogen bond to the β BChl, and a decrease in the effect of the α-BChl hydrogen bond. Thus, the change in the number of hydrogen bonds is not the major reason for the difference in the peak position. The correlation of the optical shift and the difference in the angles of the acetyl groups when comparing the BChls of LH2 and LH3 has been noted earlier (*4*).

The structural differences observed in the three-dimensional structures of LH2 and LH3 clearly indicated that the difference in the number of hydrogen-bonded BChls was not likely to be the dominant reason for the difference in their observed Q_y transition energies. However, the mutations made in the LH2 complex of *Rb. sphaeroides* provide a compelling pattern that has indicated the importance of hydrogen bonding in this complex. When applied to LH2 from *Rb. sphaeroides* using the parameters, the site energy of wild type is estimated to be 13108 cm^{-1} for both BChls. When either of the wild-type hydrogen bond donors, both Tyr residues at α44 and α45, is mutated to Phe, the resulting mutant complexes have the same Q_y transition at 11933 cm^{-1}, a 237 cm^{-1} blue shift relative to the wild-type complex (*23*, *25*). The 237 cm^{-1} blue shift can be modeled as arising from comparable changes in the site energies but predominately for different BChls, namely, ε_α and ε_β for the α44 and α45 mutants, respectively. The double mutant that changes Tyr α44 and Tyr α45 to Phe α44 and Leu α45 results in a mutant complex with a Q_y transition at 12107 cm^{-1}, a 411 cm^{-1} blue shift relative to wild type, a shift nearly double that observed for the single mutants and resulting from shifts of both site energies. The sequence and spectral similarities of the *Rps. acidophila* LH2 and LH3 complexes and the *Rb. sphaeroides* LH2 wild-type and mutant complexes have long implied a structural similarity as well, but a structural analogy between the LH3 complex and mutant *Rb. sphaeroides* LH2 complexes can no longer be easily made for the α-bound BChl, since the LH2 sequence of *Rb. sphaeroides* is incapable of maintaining the hydrogen bond as observed in the LH3 structure (Figure 4).

The LH1 mutants in this paper show a pattern of shifts indicating that the mutations made to the α and β peptides produce changes in the optical spectrum that are largely independent and additive. Such a pattern is consistent with the situation where the individual mutations affect either the α or β site energies, leaving the other site energy unchanged. Similar to the analysis of the *Rps. acidophila* complexes, the site energies for the wild-type LH1 are set to be both equal to 12858 cm^{-1} in order to yield the experimentally observed Q_y transition energy. The calculated value for the α BChl site energy of the Trp α43 to Phe mutant FLW is found to be 713 cm^{-1} greater than wild type while the Trp β48 to Phe mutant WLF has a 190 cm^{-1} shift of the β BChl site energy. These changes in the site energies yield estimated shifts of 26 nm for the FLW mutant and 7 nm for the WLF mutant, in very good agreement with the observed values of 23 and 7 nm, respectively.

The availability of LH complexes with altered cofactors provides an additional means of examining the role of the site energies. Biochemical substitution of Zn-BChl for BChl in LH1 results in a 6 nm shift, or a 100 cm^{-1} difference in the spectra (*67*), which provides an estimate of 100 cm^{-1} for the change in the site energies, ε_α and ε_β, when Zn-BChl is present compared to BChl. Based upon the measured ratio of 0.744 for extinction coefficients of isolated Zn-BChl compared to BChl (*68*), the ratio of the squared dipole moments will also be 0.744, allowing an estimate of the change in the scaling parameter C using eq 3. With these estimates for the site energies, ε_α and ε_β, and the scaling

parameter C, the σ_1, σ_2, and σ_3 parameters can be determined using eqs 7−9 to be −371.9, 0.882, and 1474260 cm^{-1}, respectively, for LH1 and $\sigma_1 = -273.2$ cm^{-1}, $\sigma_2 = -54.68$ cm^{-1}, and $\sigma_3 = 1{,}304{,}430$ cm^{-1} for LH2. Both LH1 and LH2 have been altered in a strain of *Rb. sphaeroides* containing a mutated magnesium chelatase subunit D that produces zinc bacteriochlorophyll (Zn-BChl) instead of the normal magnesium-containing BChl (*69*−*71*). For the monomeric BChls near 800 nm in LH2, the difference in the energies of the Q_y transition moments should be 6 nm, or 794 nm for the Zn-BChl mutant. For the coupled BChls at 850 nm in LH2 and 875 nm in LH1, these parameters yield differences in the transition energies (eq 12) of 143 and 181 cm^{-1}, or 840 and 861 nm for the Zn-BChl-containing LH2 and LH1, respectively. These calculated peak values are in excellent agreement with the observed peaks at 793, 836, and 859 nm for the Zn-BChl-containing LH1 and LH2 complexes. The agreement of the observed and calculated peaks provides additional support for the utility of these relationships to understand the light-harvesting complexes.

CONCLUSIONS

Overall, these relationships provide a framework in which the electronic structure of BChls, models provided by the existing LH structures, and the observed Q_y transition energies for mutant LH complexes can be linked together in terms of structural changes, in particular acetyl group rotations, and hydrogen-bonding alterations. Mutations that affect the hydrogen bonding to the BChls in the LH complexes of purple bacteria have long been correlated with shifts in their absorption spectra. In this paper it is shown that changing Leu α44 of the LH1 complex of *Rb. sphaeroides* has a significant effect on the absorption spectrum of the complex. The mutation from Leu to Tyr, which produces a 4 nm blue shift and a resonance Raman spectrum with a significant alteration to the hydrogen bonding of the C3-acetyl groups of the BChl pigments, indicates that a hydrogen bond donor at this position is capable of forming a hydrogen bond to the α-bound BChl. The mutation from Leu to Phe produces a similar blue shift of 5 nm but results in a resonance Raman spectrum that shows no change to the hydrogen bonding of the C3-acetyl groups of the BChl pigments, indicating that shifts in the absorption spectrum can be produced solely from structural changes. When these mutations are performed in conjunction with the previously reported mutations Trp α43 to Phe and Trp *β*48 to Phe, a consistent picture showing the dependence of the absorption spectrum on the hydrogen bonding of the C3-acetyl group emerges, but also showing that shifts in the absorption spectra of these mutants have to be considered as being due to structural changes as well as hydrogen bond changes. These spectral changes are interpreted in models in which the mutations result in both a structural contribution, which is modeled in terms of a rotation of the acetyl groups, and a contribution from a loss or gain of a hydrogen bond. A relationship is also developed that links the effects of acetyl group rotations and hydrogen bonding to the Q_y transition energy of individual BChl molecules along with a relatively simple equation that incorporates this change in site energy to produce the change in the Q_y transition energy of the LH complex. This interpretation of the optical shifts in terms of alterations of the site energies of the individual BChls requires the assumption of a symmetrical arrangement of the proteins forming the LH1 complex. An asymmetry of the LH1 complex, due to a combination of PufX and disorder, could be incorporated, but the lack of consensus in these features, such as the value of the disorder parameters, makes use of the derived parameters problematic. While the spectral changes most likely arise from a number of structural changes, including alterations of the disorder of the complex, that cannot be directly modeled at present, the assumption of a symmetrical ring shows that the spectral changes can be interpreted in terms of rotations of the acetyl groups that yield reasonable changes in angles.

ACKNOWLEDGMENT

The coordinates of the LH1 model were provided by Dr. Klaus Schulten and Dr. Xiche Hu. We thank the RTG group for assistance with the initial efforts of this project and Alicia Kishpaugh for assistance with the size-exclusion measurements.

REFERENCES

1. Hunter, N., Daldal, F., Thurnauer, M., and Beatty, J. T., Eds. (2008) The Purple Phototrophic Bacteria, Springer-Verlag, Dordrecht, The Netherlands.
2. Cogdell, R. J., Howard, T. D., Isaacs, N. W., McLuskey, K., and Gardiner, A. T. (2002) Structural factors which control the position of the Q_y absorption band of bacteriochlorophyll *a* in purple antenna complexes. *Photosynth. Res. 74*, 135–141.
3. Cogdell, R. J., Gardiner, A. T., Roszak, A. W., Law, C., Southall, J., and Isaacs, N. W. (2004) Rings, ellipses, and horseshoes: how purple bacteria harvest solar energy. *Photosynth. Res. 81*, 207–214.
4. Cogdell, R. J., Gall, A., and Köhler, J. (2006) The architecture and function of the light-harvesting apparatus of purple bacteria: from single molecules to *in vivo* membranes. *Q. Rev. Biophys. 39*, 227–324.
5. Silber, M. V., Gabriel, G., Strohmann, B., Garcia-Martin, A., Robert, B., and Braun, P. (2008) Fine tuning the spectral properties of LH2 by single amino acid residues. *Photosynth. Res. 96*, 145–151.
6. Deisenhofer, J., Epp, O., Miki, K., Huber, R., and Michel, H. (1985) Structure of the protein subunits in the photosynthetic reaction centre of *Rhodopseudomonas viridis* at 3 Å resolution. *Nature 318*, 618–624.
7. Allen, J. P., Feher, G., Yeates, T. O., Komiya, H., and Rees, D. C. (1987) Structure of the reaction center from *Rhodobacter sphaeroides* R-26: the cofactors. *Proc. Natl. Acad. Sci. U.S.A. 84*, 5730–5734.
8. McDermott, G., Prince, S. M., Freer, A. A., Hawthornthwaite-Lawless, A. M., Papiz, M. Z., Cogdell, R. J., and Isaacs, N. W. (1995) Crystal structure of an integral membrane light-harvesting complex from photosynthetic bacteria. *Nature 374*, 517–521.
9. Koepke, J., Hu, X., Muenke, C., Schulten, K., and Michel, H. (1996) The crystal structure of the light-harvesting complex II (B800−850) from *Rhodospirillum molischianum*. *Structure 4*, 581–597.
10. McLuskey, K., Prince, S. M., Cogdell, R. J., and Isaacs, N. W. (2001) The crystallographic structure of the B800−820 LH3 light-harvesting complex from the purple bacteria *Rhodopseudomonas acidophila* strain 7050. *Biochemistry 40*, 8783–8789.
11. Karrasch, S., Bullough, P. A., and Ghosh, R. (1995) The 8.5 Å projection map of the light-harvesting complex I from *Rhodospirillum rubrum* reveals a ring composed of 16 subunits. *EMBO J. 14*, 631–638.
12. Farchaus, J. W., and Oesterhelt, D. (1989) A *Rhodobacter sphaeroides* puf L, M and X deletion mutant and its complementation in *trans* with a 5.3 kb *puf* operon shuttle fragment. *EMBO J. 8*, 47–54.
13. Barz, W. P., Francia, F., Venturoli, G., Melandri, B. A., Vermeglio, A., and Oesterhelt, D. (1995) Role of the PufX protein in photosynthetic growth of *Rhodobacter sphaeroides*. 1. PufX is required for efficient light-driven electron transfer and photophosphorylation under anaerobic conditions. *Biochemistry 34*, 15235–15247.
14. Barz, W. P., Vermeglio, A., Francia, F., Venturoli, G., Melandri, B. A., and Oesterhelt, D. (1995) Role of the PufX protein in photosynthetic growth of *Rhodobacter sphaeroides*. 2. PufX is required for the efficient ubiquinone/ubiquinol exchange between the reaction center Q_B site and the cytochrome bc_1 complex. *Biochemistry 34*, 15248–15258.
15. Parkes-Loach, P. S., Law, C. J., Recchia, P. A., Kehoe, J., Nehrlich, S., Chen, J., and Loach, P. A. (2001) Role of the core region of the PufX protein in inhibition of reconstitution of the core light-harvesting complexes of *Rhodobacter sphaeroides* and *Rhodobacter capsulatus*. *Biochemistry 40*, 5593–5601.
16. Bahatyrova, S., Frese, R. N., van der Werf, K. O., Otto, C., Hunter, C. N., and Olsen, J. D. (2004) Flexibility and size heterogeneity of the

LH1 light harvesting complex revealed by atomic force microscopy. *J. Biol. Chem. 279*, 21327–21333.
17. Bahatyrova, S., Frese, R. N., Siebert, C. A., Olsen, J. D., van der Werf, K. O., van Grondelle, R., Niederman, R. A., Bullough, P. A., Otto, C., and Hunter, C. N. (2004) The native architecture of a photosynthetic membrane. *Nature 430*, 1058–1062.
18. Scheuring, S., Levy, D., and Rigaud, J. L. (2006) Watching the components of photosynthetic bacterial membranes and their in situ organization by atomic force microscopy. *Biochim. Biophys. Acta 1712*, 109–127.
19. Roszak, A. W., Howard, T. D., Southall, J., Gardiner, A. T., Law, C. J., Isaacs, N. W., and Cogdell, R. J. (2003) Crystal structure of RC-LH1 core complex from *Rhodopseudomonas palustris*. *Science 302*, 1969–1972.
20. Germeroth, L., Lottspeich, F., Robert, B., and Michel, H. (1993) Unexpected similarities of the B800−850 light-harvesting complex from *Rhodospirillum molischianum* to the B870 light-harvesting complexes from other purple photosynthetic bacteria. *Biochemistry 32*, 5615–5621.
21. Sturgis, J. N., Olsen, J. D., Robert, B., and Hunter, C. N. (1997) Functions of conserved tryptophan residues of the core light-harvesting complex of *Rhodobacter sphaeroides*. *Biochemistry 36*, 2772–2778.
22. Olsen, J. D., Sockalingum, G. D., Robert, B., and Hunter, C. N. (1994) Modification of a hydrogen bond to a bacteriochlorophyll *a* molecule in the light-harvesting 1 antenna of *Rhodobacter sphaeroides*. *Proc. Natl. Acad. Sci. U.S.A. 91*, 7124–7128.
23. Fowler, G. J. S., Visschers, R. W., Grief, G. G., van Grondelle, R., and Hunter, C. N. (1992) Genetically modified photosynthetic antenna complexes with blue-shifted absorption bands. *Nature 355*, 848–850.
24. Fowler, G. J. S., Sockalingum, G. D., Robert, B., and Hunter, C. N. (1994) Blue shifts in bacteriochlorophyll absorbance correlate with changed hydrogen bonding patterns in light-harvesting 2 mutants of *Rhodobacter sphaeroides* with alterations at α-Tyr-44 and α-Tyr-45. *Biochem. J. 299*, 695–700.
25. Hess, S., Visscher, K. J., Pullerits, T., Sundström, V., Fowler, G. J. S., and Hunter, C. N. (1994) Enhanced rates of subpicosecond energy transfer in blue-shifted light harvesting LH2 mutants of *Rhodobacter sphaeroides*. *Biochemistry 33*, 8300–8305.
26. Gall, A., Fowler, G. J. S., Hunter, C. N., and Robert, B. (1997) Influence of the protein binding site on the absorption properties of the monomeric bacteriochlorophyll in *Rhodobacter sphaeroides* LH2 complex. *Biochemistry 36*, 16282–16287.
27. Hanson, L. K., Thompson, M. A., and Fajer, J. (1987) Environmental effects on the properties of chlorophylls *in vivo* theoretical models, in Progress in Photosynthesis Research (Biggens, J., Ed.) Vol. *1*, pp I.3.311−I.3.314, Martinus Nijhoff, Dordecht, The Netherlands.
28. Sturgis, J. N., Jirsakova, V., Reiss-Husson, F., Cogdell, R. J., and Robert, B. (1995) Structure and properties of the bacteriochlorophyll binding site in peripheral light-harvesting complexes of purple bacteria. *Biochemistry 34*, 517–523.
29. Gudowska-Nowak, E., Newton, M. D., and Fajer, J. (1990) Conformational and environmental effects on bacteriochlorophyll optical spectra: correlation of calculated spectra with structural results. *J. Phys. Chem. 94*, 5795–5801.
30. Yanisch-Perron, C., Vieira, J., and Messing, J. (1985) Improved M13 phage cloning vectors and host strains: nucleotide sequences of the M13mp18 and pUC19 vectors. *Gene 33*, 103–119.
31. Keen, N. T., Tamaki, S., Kobayashi, D., and Trollinger, D. (1988) Improved broad-host-range plasmids for DNA cloning in Gram-negative bacteria. *Gene 70*, 191–197.
32. Simon, R., Priefer, U., and Puehler, A. (1983) A broad host range mobilization system for *in vivo* genetic engineering: transposon mutagenesis in Gram-negative bacteria. *BioTechnology 1*, 784–791.
33. Williams, J. C., and Taguchi, A. K. W. (1995) Genetic manipulation of purple photosynthetic bacteria, in Anoxygenic Photosynthetic Bacteria (Blankenship, R. E., Madigan, M. T., and Bauer, C. E., Eds.) pp 1029−1065, Kluwer Academic, Dordrecht, The Netherlands.
34. Bachmann, R. C., Tadros, M. H., Oelze, J., and Takemoto, J. Y. (1983) Purification and characterization of the B875 light-harvesting complex of *Rhodopseudomonas sphaeroides*. *Biochem. Int. 7*, 629–634.
35. Mattioli, T. A., Lin, X., Allen, J. P., and Williams, J. C. (1995) Correlation between multiple hydrogen bonding and alteration of the oxidation potential of the bacteriochlorophyll dimer of reaction centers from *Rhodobacter sphaeroides*. *Biochemistry 34*, 6142–6152.
36. Hu, X., and Schulten, K. (1998) Model for the light-harvesting complex I (B875) of *Rhodobacter sphaeroides*. *Biophys. J. 75*, 683–694.
37. Geyer, T. (2007) On the effects of PufX on the absorption properties of the light-harvesting complexes of *Rhodobacter sphaeroides*. *Biophys. J. 93*, 4374–4381.
38. Sebban, P., Robert, B., and Jolchine, G. (1985) Isolation and spectroscopic characterization of the B875 antenna complex of a mutant of *Rhodopseudomonas sphaeroides*. *Photochem. Photobiol. 42*, 573–578.
39. Broglie, R. M., Hunter, C. N., Delepelaire, P., Niederman, R. A., Chua, N. H., and Clayton, R. K. (1980) Isolation and characterization of the pigment-protein complexes of *Rhodopseudomonas sphaeroides* by lithium dodecyl sulfate/polyacrylamide gel electrophoresis. *Proc. Natl. Acad. Sci. U.S.A. 77*, 87–91.
40. Hunter, C. N., Pennoyer, J. D., Sturgis, J. N., Farrelly, D., and Niederman, R. (1988) Oligomerization states and associations of light-harvesting pigment-protein complexes of *Rhodobacter sphaeroides* as analyzed by lithium dodecyl sulfate-polyacrylamide gel electrophoresis. *Biochemistry 27*, 3459–3467.
41. Linnanto, J., and Korppi-Tommola, J. (2004) Structural and spectroscopic properties of Mg-bacteriochlorin and methyl bacteriochlorophyllides *a*, *b*, *g*, and *h* studied by semiempirical, ab initio, and density functional molecular orbital methods. *J. Phys. Chem. A 108*, 5872–5882.
42. He, Z., Sundström, V., and Pullerits, T. (2002) Influence of the protein binding site on the excited states of bacteriochlorophyll: DFT calculations of B800 in LH2. *J. Phys. Chem. B 106*, 11606–11612.
43. Tronrud, D. E., Schmid, M. F., and Matthews, B. W. (1986) Structure and X-ray amino acid sequence of a bacteriochlorophyll *a* protein from *Prosthecochloris aestuarii* refined at 1.9 Å resolution. *J. Mol. Biol. 188*, 443–454.
44. Li, Y. F., Zhou, W. L., Blankenship, R. E., and Allen, J. P. (1997) Crystal structure of the bacteriochlorophyll *a* protein from *Chlorobium tepidum*. *J. Mol. Biol. 271*, 456–471.
45. Camara-Artigas, A., Blankenship, R., and Allen, J. P. (2003) The structure of the FMO protein from *Chlorobium tepidum* at 2.2 Å resolution. *Photosynth. Res. 75*, 49–55.
46. Robert, B. (2009) Spectroscopic properties of antenna complexes from purple bacteria, in The Purple Phototrophic Bacteria (Hunter, C. N., Daldal, F., Thurnauer, M., and Beatty, J. T., Eds.) pp 199−212, Springer-Verlag, Dordrecht, The Netherlands.
47. Parson, W. W., and Warshel, A. (1987) Spectroscopic properties of photosynthetic reaction centers. 2. Application of the theory to *Rhodopseudomonas viridis*. *J. Am. Chem. Soc. 109*, 6152–6163.
48. Linnanto, J., and Korppi-Tommola, J. (2006) Quantum chemical simulation of excited states of chlorophylls, bacteriochlorophylls, and their complexes. *Phys. Chem. Chem. Phys. 8*, 663–687.
49. Kunieda, M., Mizoguchi, T., and Tamiaki, H. (2004) Diastereoselective self-aggregation of synthetic 3-(1-hydroxyethyl)-bacteriopyrochlorophyll-*a* as a novel photosynthetic antenna model absorbing near the infrared region. *Photochem. Photobiol. 79*, 55–61.
50. Olsen, J. D., Sturgis, J. N., Westerhuis, W. H. J., Fowler, G. J. S., Hunter, C. N., and Robert, B. (1997) Site-directed modification of the ligands to the bacteriochlorophylls of the light-harvesting LH1 and LH2 complexes of *Rhodobacter sphaeroides*. *Biochemistry 36*, 12625–12632.
51. Kwa, L. G., Garcia-Martin, A., Vegh, A. P., Strohmann, B., Robert, B., and Braun, P. (2004) Hydrogen bonding in a model bacteriochlorophyll-binding site drives assembly of light harvesting complexes. *J. Biol. Chem. 279*, 15067–15075.
52. Barkigia, K. M., Chantranupong, L., Smith, K. M., and Fajer, J. (1988) Structural and theoretical models of photosynthetic chromophores. Implications for redox, light absorption properties and vectorial electron flow. *J. Am. Chem. Soc. 110*, 7566–7567.
53. Prince, S. M., Papiz, M. Z., Freer, A. A., McDermott, G., Hawthornthwaite-Lawless, A. M., Cogdell, R. J., and Isaacs, N. W. (1997) Apoprotein structure in the LH2 complex from *Rhodopseudomonas acidophila* strain 10050: modular assembly and protein pigment interactions. *J. Mol. Biol. 268*, 412–423.
54. Papiz, M. Z., Prince, S. M., Howard, T., Cogdell, R. J., and Isaacs, N. W. (2003) The structure and thermal motion of the B800−850 LH2 complex from *Rps. acidophila* at 2.0 Å resolution and 100K: New structural features and functionally relevant motions. *J. Mol. Biol. 326*, 1523–1538.
55. Lapouge, K., Naveke, A., Gall, A., Ivancich, A., Seguin, J., Scheer, H., Sturgis, J. N., Mattioli, T. A., and Robert, B. (1999) Conformation of bacteriochlorophyll molecules in photosynthetic proteins from purple bacteria. *Biochemistry 38*, 11115–11121.
56. Miller, K. R. (1982) Three-dimensional structure of a photosynthetic membrane. *Nature 300*, 53–55.
57. Gerken, U., Lupo, D., Tietz, C., Wrachtrup, J., and Ghosh, R. (2003) Circular symmetry of the light-harvesting 1 complex from *Rhodospirillum rubrum* is not perturbed by interaction with the reaction center. *Biochemistry 42*, 10354–10360.

58. Stahlberg, H., Dubochet, J., Vogel, H., and Ghosh, R. (1998) Are the light-harvesting I complexes from *Rhodospirillum rubrum* arranged around the reaction center in a square geometry? *J. Mol. Biol. 282*, 819–831.
59. Siebert, C. A., Qian, P., Fotiadis, D., Engel, A., Hunter, C. N., and Bullough, P. A. (2004) Molecular architecture of photosynthetic membranes in *Rhodobacter sphaeroides*: the role of PufX. *EMBO J. 23*, 690–700.
60. van Mourik, F., Visschers, R. W., and van Grondelle, R. (1992) Energy transfer and aggregate effects in the inhomogeneously broadened core light-harvesting complex of *Rhodobacter sphaeroides*. *Chem. Phys. Lett. 193*, 1–7.
61. Georgakopoulou, S., Frese, R. N., Johnson, E., Koolhaas, C., Cogdell, R. J., van Grondelle, R., and van der Zwan, G. (2002) Absorption and CD spectroscopy and modeling of various LH2 complexes from purple bacteria. *Biophys. J. 82*, 2184–2197.
62. Aklujkar, M., and Beatty, J. T. (2005) The PufX protein of *Rhodobacter capsulatus* affects the properties of bacteriochlorophyll *a* and carotenoid pigments of light-harvesting complex I. *Arch. Biochem. Biophys. 443*, 21–32.
63. Richter, M. F., Baier, J., Prem, T., Oellerich, S., Francia, F., Venturoli, G., Oesterhelt, D., Southall, J., Cogdell, R. J., and Kohler, J. (2007) Symmetry matters for the electronic structure of core complexes from *Rhodopseudomonas palustris* and *Rhodobacter sphaeroides* $PufX^{-}$. *Proc. Natl. Acad. Sci. U.S.A. 104*, 6661–6665.
64. Sturgis, J. N., Gall, A., Ellervee, A., Freiberg, A., and Robert, B. (1998) The effect of pressure on the bacteriochlorophyll *a* binding sites of the core antenna complex of *Rhodosprillum rubrum*. *Biochemistry 37*, 14875–14880.
65. Timpmann, K., Ellervee, A., Pullerits, T., Ruus, R., Sundstrom, V., and Freiberg, A. (2001) Short-range exciton couplings in LH2 photosynthetic antenna proteins studies by high hydrostatic pressure absorption spectroscopy. *J. Phys. Chem. B 105*, 8436–8444.
66. Kangur, L., Timpmann, K., and Freiberg, A. (2008) Stability of integral membrane proteins under high hydrostatic pressure: the LH2 and LH3 antenna pigment-protein complexes from photosynthetic bacteria. *J. Phys. Chem. B 112*, 7948–7955.
67. Lapouge, K., Naveke, A., Robert, B., Scheer, H., and Sturgis, J. N. (2000) Exchanging cofactors in the core antennae from purple bacteria: structure and properties of Zn-bacteriopheophytin-containing LH1. *Biochemistry 39*, 1091–1099.
68. Hartwich, G., Fiedor, L., Simonin, I., Cmiel, E., Schafer, W., Noy, D., Scherz, A., and Scheer, H. (1998) Metal-substituted bacteriochlorophylls. 1. Preparation and influence of metal and coordination on spectra. *J. Am. Chem. Soc. 120*, 3675–3683.
69. Wendling, M., Lapouge, K., van Mourik, F., Novoderezhkin, V., Robert, B., and van Grondelle, R. (2002) Steady-state spectroscopy of zinc-bacteriopheophytin containing LH1- an in vivo and in silico study. *Chem. Phys. 275*, 31–45.
70. Jaschke, P. R., and Beatty, J. T. (2007) The photosystem of *Rhodobacter sphaeroides* assembles with zinc bacteriochlorophyll in a *bchD* (magnesium chelatase) mutant. *Biochemistry 46*, 12491–12500.
71. Lin, S., Jaschke, P. R., Wang, H., Paddock, M., Tufts, A., Allen, J. P., Rosell, F. I., Mauk, A. G., Woodbury, N. W., and Beatty, J. T. (2009) Electron transfer in *Rhodobacter sphaeroides* reaction centers assembled with zinc bacteriochlorophylls. *Proc. Natl. Acad. Sci. U.S.A. 106*, 8537–8542.